平成25年度厚生労働科学研究費補助金（認知症対策総合研究事業）
「BPSDの症状評価法および治療法の開発と脳内基盤解明を目指した総合的研究」
分担研究報告書
サブタイトル：高齢者における精神病性障害の病理基盤
研究分担者　　横田　修　（所属名）きのこエスポアール病院精神科

○研究要旨

高齢者に認められる幻覚妄想状態を主徴とし認知症を欠く統合失調症様精神病性障害（late-onset schizophrenia and psychotic disorders: LOSD）に関係する病理学的背景を探索的に検討するため，40才以降にLOSDを初発した23例，精神症状や運動障害を欠く臨床的正常対照71例,40才以降にLOSD以外の精神疾患を初発した疾患対照22例を組織病理学的に検討した．LOSD全例（対正常対照群）において，レビー小体病（LBD）は26.1％（11.3％），嗜銀顆粒病（AGD）は21.7％（8.5％），皮質基底核変性症（CBD）は4.3％（0.0％）であった．病理学的にアルツハイマー病（AD）の診断基準を満たす例はなかった．LOSD群におけるLBD，AGD，CBDの合計頻度は正常対照群より有意に高かった．AGDの重症度はLOSD群において正常対照群より有意に高度であったが，CBDにAGDを合併した例を除く全てのAGD例ではそのタウ病変が辺縁系と隣接する側頭葉皮質に留まっていた．65歳以上発症のLOSD症例ではLBDは36.4％（19.4％），嗜銀顆粒病は36.4％（8.3％）で，AGDは年齢をマッチさせた正常対照群より有意に高頻度であった．65歳未満発症のLOSDではLBD，AGD，CBDの頻度は16.7%，8.3%，8.3％で，これらは正常対照群よりやや高いが統計学的には有意差がなかった（10.2%，5.1%，0.0％）．以上の結果はAGDは65歳以上で初発するLOSDと関係する事を示唆している．

A.研究目的

高齢者に認められる幻覚妄想状態を主徴とし認知症を欠く統合失調症様精神病性障害（late-onset schizophrenia and psychotic disorders: LOSD）に関係する病理学的背景を探索的に検討する．

B.研究方法

40才以降にLOSDを初発した23例,精神症状や運動障害を欠く正常対照例71例,40才以降にLOSD以外の精神疾患を初発した22例を組織病理学的に検討した．全例のホルマリン固定パラフィン包埋したブロックから一般染色用に10μm厚，免疫染色用には6μm厚の切片を作成し，前頭葉,側頭葉,頭頂葉,後頭葉,基底核,中脳,橋,延髄,小脳のパラフィン包埋切片をH&E,Klüver-Barrera,Gallyas銀，Bielschowsky銀染色，およびリン酸化タウ（AT8，mouse，monoclonal，1:1,000,Innogenetics,Ghent,Belgium),タウ(T46:mouse,monoclonal,1:1,000,Invitrogen,Carlsbad,CA,USA),three-repeat(3R)tau(RD3:mouse,monoclonal,1:3,000,Upstate,Syracuse,NY,USA),four-repeat(4R)tau(RD4:mouse,monoclonal,1:200,Upstate),Aβ11-28(12B2,mouse,monocloncal,1:2,000,Immuno-BiologicalLaboratories,Fujioka,Japan),Aβ42(Aβ42,rabbit,polyclonal,1:100,Immuno-BiologicalLaboratories),リン酸化α-synuclein(psyn#64,mouse,

monoclonal, 1:5,000, Wako, Osaka, Japan), α-synuclein (anti-α-synuclein, mouse monoclonal, 1:10,000, Invitrogen, Burlington, ON, Canada), リン酸化 TDP-43 (pS409/410-2, rabbit polyclonal, 1:5,000, Cosmo Bio, Tokyo, Japan), TDP-43 (anti-TDP-43, rabbit polyclonal, 1:1,000, ProteinTech, Chicago, IL, USA), リン酸化 neurofilament (SMI31, mouse, monoclonal IgG, 1:10,000, Sternberger Monoclonals, Baltimore, MD, USA) を用いた免疫染色を行った.

病変の評価は以下の標準的な方法で行った. (1) 神経原線維変化は AT8 染色標本上で Braak stage (stage 0-VI) を用いた. (2) 老人斑の分布は Aβ 染色を用いて Braak stage (stage 0, A, B, C) で評価した. アルツハイマー病の病理診断は NIA-Reagan criteria で行った. (3) レビー小体関連病理はコンセンサスガイドライン第 3 版に基づく脳幹型, 辺縁系型, 新皮質型と, 後に報告された扁桃核型の 4 型に分類した. (4) 嗜銀顆粒病のステージは Saito's AGD stage (stage 0-III) に基づいて分類した. (5) 進行性核上性麻痺 (PSP) の診断は診断基準に加えて tufted astrocytes を有している症例とした. 皮質基底核変性症 (CBD) は astrocytic plaques の存在を必須とした. (6) TDP-43-positive lesions 辺縁系, 側頭葉皮質, 舌下神経核で評価し, 扁桃核型, 辺縁系型, 新皮質型に分類した. (7) 神経細胞脱落は H&E と KB 染色を用いて軽度, 中等度, 高度に分類した. 血管障害は精神疾患症例について左半球で評価した. 統計解析は Mann-Whitney U test, Fisher's exact test を用いて群間比較した. 多重比較は Bonferroni 補正を行った. $P<0.05$ を有意とした.

(倫理面への配慮)

剖検に際して家族から書面で同意を得た. 研究計画について岡山大学倫理委員会の承認を得た.

C. 研究結果

- LOSD 全例 (対正常対照群) において, レビー小体病 (LBD) は 26.1 % (11.3 %), 嗜銀顆粒病 (AGD) は 21.7 % (8.5 %), 皮質基底核変性症 (CBD) は 4.3 % (0.0 %) であった. 病理学的にアルツハイマー病 (AD) の診断基準を満たす例はなかった.
- LOSD 群における LBD, AGD, CBD の合計頻度は正常対照群より有意に高かった.
- AGD の重症度は LOSD 群において正常対照群より有意に高度であったが, CBD に AGD を合併した例を除く全ての AGD 例ではそのタウ病変が辺縁系と隣接する側頭葉皮質に留まっていた.
- 65 歳以上発症の LOSD 症例では LBD は 36.4 % (19.4 %), 嗜銀顆粒病は 36.4 % (8.3 %) で, AGD は年齢をマッチさせた正常対照群より有意に高頻度であった.
- 65 歳未満発症の LOSD では LBD, AGD, CBD の頻度は 16.7%, 8.3%, 8.3 %で, 正常対照群 (10.2%, 5.1%, 0.0 %) よりやや高い傾向があったが統計学的には有意差はなかった.
- 全ての精神疾患患者のみで病変と臨床症状の関係を解析すると, AGD 群における妄想の頻度は軽微な AD 病理しか有さない精神疾患症例群 (Braak NFT stage I-II, Braak SP stage 0-A のみで LBD, AGD, CBD, PSP, TDP43 病理を欠く例) に比べて有意に高頻度であった.

D. 考察

認知症を有する AGD の一部の症例は妄想, 幻覚, 攻撃性, 易刺激性, 強迫といった様々な精神症状を呈する事が報告されてきた. しかしながら我々の知る限り認知症のない LOSD と AGD の関係を示した報告は過去にない. 一般的に言って, 若年発症の精神症状と組織病理学的変化の因果関

係を証明する事は難しい．なぜなら組織病理学的変化は死亡時に存在するものであり，精神症状は死亡の何十年も前に出現していたものであるので時間的な点で因果関係が言及しにくく，かつ，主要な組織病理学的変化は加齢と共に増加するということも死亡時の病理の頻度を考える際には考慮する必要がある．しかし我々の検討は，臨床的に健常な高齢者に比べて有意に AGD が高頻度である事を示していることから，LOSD において認められた高頻度の AGD は死亡時年齢の影響では説明できないと考えられる．

我々の LOSD 症例群における AGD の程度は，その解剖学的分布の点で過去に報告された認知症を呈する AGD 例のそれよりも軽い．例えば認知症を呈する AGD 例ではその分布ステージは新皮質に達しているステージ III が通常である事が報告されているが，我々の LOSD 症例においてはそのステージは I かステージ II である．このため我々の LOSD を呈した AGD 例のタウ病理が軽度で，かつ，少なくとも経過の中期まで認知症を欠いていたということは自然であると考えられる．この様な軽度から中等度の AGD 病理が気分，不安，思考といった精神機能にどのような影響を与えるのかはこれまでほとんど研究されていない．我々の結果は認知症を欠く LOSD は少なくとも軽度から中等度の AGD 症例の臨床表現型の一つである可能性を示している．精神病性エピソードは脳血管障害，頭部外傷，てんかんといった辺縁系や隣接する側頭葉皮質が障害される病態で出現しうる事が知られている．これらの知見を踏まえると，AGD における精神症状の出現は，その嗜銀顆粒が辺縁系を中心に存在することに関係しているのかもしれない．一部の LBD 症例は構築された妄想を示し，その頻度はパーキンソン病では 17-30%，レビー小体型認知症では 25-28.6 %と報告されている．我々の検討でも LBD の頻度は LOSD において正常対照群より 2.5 倍高頻度であり，発症年齢が 65 歳以上のうつ病症例においては正常対照群より有意に高頻度であった．我々のうつ病症例においては AGD は認められなかったが，検討したサンプルサイズが小さいため，LBD の臨床スペクトラムと AGD の臨床スペクトラムが異なるのかどうかは今回の結果からは結論できない．ただし，一般的に言って変性疾患の病変の解剖学的分布は通常臨床表現と密接に関係するが，LBD と AGD とでは病変分布は異なっており，それゆえこの二疾患の精神神経学的臨床表現のスペクトラムは異なる可能性はある．例えば LBD においては辺縁系と幾つかの脳幹諸核（例えば raphe 核や青斑核）が高頻度に障害されるが，嗜銀顆粒病ではタウ病理は辺縁系に出現するが脳幹諸核にはほとんど出現しない．辺縁系や脳幹諸核の機能障害はうつ病に関係すると報告されている．AGD で LOSD 以外の精神疾患の臨床表現の頻度が高まるのかは更に多数例を対象とした検討で明らかにされるべきである．

我々の検討では LOSD の一部の例は CBD 病理を有していた．過去の検討では病理学的に確定された CBD 症例が生前に精神病性症状を有する事は稀であるとされている．興味深い事に，我々の病理学的に CBD と診断され生前に LOSD を呈した症例の発症年齢は 65 歳未満であり，これは AGD や LBD における LOSD の発症年齢が高い事と対照的であった．これらの結果に基づくと，精神科実地においては CBD は，発症年齢が 65 才以上の LOSD 例よりも，発症年齢が 65 才未満の LOSD 例で予想すべき病理背景の一つなのかもしれない．CBD 症例において LOSD が出現する病態メカニズムは不明である．ただし，AGD の共存が全ての CBD 症例に認められており，これが LOSD の出現に関与した可能性はあるだろう．

過去の幾つかの検討では，LOSD は高度の AD 病理（Braak NFT stage V-VI）とは関係していな

い事が示されてきた．これは本研究でも支持された．しかし，辺縁系における中等度の神経原線維変化（Braak NFT stage III-IV）とLOSDの関係に関する過去の知見は，必ずしも否定的な物ばかりではない.例えば,海馬や側頭葉皮質の神経原線維変化の程度は若年発症の統合失調症とLOSD症例で有意な差がなかったという報告がある一方，辺縁系に分布する中等度の神経原線維変化（Braak stage III-IV）がLOSDに関連したという報告もある．我々の検討では，LOSDにおけるBraak NFT stageは年齢をマッチさせた正常群より有意に高かったが，この結果は過去の報告と単純に比べる事はできない．なぜなら，過去の検討では神経原線維変化以外の様々な代表的な病理，例えばレビー小体，嗜銀顆粒，PSP病理，CBD病理といったものを同時に検討している報告はないからである．例えば，我々のLOSD症例では神経原線維変化のBraak stageは正常群より高かったが，これはLOSDにおいて単純に神経原線維変化が関係している可能性と，LBD，AGD，CBDといった神経原線維変化を伴う症例の頻度が高かった事を反映している可能性の両方が検討されるべきであろう．ただし，我々のLOSD症例においては，Braak stage III-IVの中等度の神経原線維変化のみを有している症例の頻度は8.7%と高くはなかったが，正常対象と比べると高い傾向があった（1.4％）．これらの知見に基づくと，辺縁系に分布するBraak stage III-IVの中等度の神経原線維変化によって説明できるLOSD症例は低頻度ながら存在する可能性があると思われる．ただしその頻度はLOSD全体の中では高くはないだろうとも考えられる．

本研究ではLOSD患者は多様な病理背景を有しており，そこにはAGDが含まれる事が明らかとなったが，生前にLOSD患者のその病理背景を予測する事は未だ難しい．今回の結果は，臨床での実用に向けて検討が進められているタウオパチーやシヌクレイノパチーのバイオマーカーがLOSD患者の背景病理の予測に有用である可能性を示唆している．より正確なLOSD患者の理解と治療戦略の開発のためには，臨床病理学的知見の更なる蓄積が待たれる．

E. 結論

AGD病変の高度な例における代表的な臨床表現には易怒性を伴う認知症が知られてきたが，今回の結果は，LOSDは軽度から中等度のAGD症例の臨床表現の一つである可能性を示唆している．AGDの病変が最初に迂回回と扁桃核におこり、隣接する側頭葉皮質に広がるという進展様式は、比較的軽度のAGDを有する患者が認知症になる前に精神症状を呈することに関係するかもしれない．

F. 研究発表

1. 論文発表

Nagao S, Yokota O, Ikeda C, Takeda N, Ishizu H, Kuroda S, Sudo K, Terada S, Murayama S, Uchitomi Y. Argyrophilic grain disease as a neurodegenerative substrate in late-onset schizophrenia and delusional disorders. Eur Arch Psychiatry Clin Neurosci. (In press)

2. 学会発表

長尾茂人，横田 修，池田智香子，大島悦子，石津秀樹，黒田重利，森定ゆみ，須藤浩一郎，中島良彦，寺田整司，内富庸介．晩発性精神病性障害:神経変性疾患の頻度と重症度について
第54回　日本神経病理学会総会，東京．2013.4.25-4.26

H. 知的財産権の出願・登録状況（予定を含む）

1. 特許取得

なし

2. 実用新案登録

なし

3. その他

なし

Ⅲ.　研究成果の刊行に関する一覧表

別紙４

研究成果の刊行に関する一覧表レイアウト（参考）

書籍

著者氏名	論文タイトル名	書籍全体の編集者名	書　籍　名	出版社名	出版地	出版年	ページ
新井哲明	抗認知症薬および脳循環・代謝改善薬	樋口輝彦	精神・神経の治療薬事典	総合医学社	東京	2013	300-305
新井哲明	ピック病型認知症	岡崎祐士	ICD-10精神科診断ガイドブック	中山書店	東京	2013	49-63
池田　学	脳の理解	浦上克哉，川瀬康裕，児玉直樹	認知症予防専門士テキストブック	徳間書店	東京	2013	12-16
池田　学	前頭側頭型認知症	北川泰久，寺本　明，三村　將	神経・精神疾患診療マニュアル	日本医師会	東京	2013	199-200
池田　学	認知症	平山恵造，田川皓一	脳血管障害と神経心理学　第２版	医学書院	東京	2013	77-82
池田　学，小松優子	認知症とケア	池田　学	脳とこころのプライマリケア２　知能の衰え	シナジー	東京	2013	51-56
池田　学	前頭側頭葉変性症（含：進行性失語症）	井村裕夫	第４版わかりやすい内科学	文光堂	東京	2014	600-601
松崎志保，橋本　衛，池田　学	梅毒	朝田　隆	誤診症例から学ぶ　認知症とその他の疾患の鑑別	医学書院	東京	2013	156−167
烏帽子田彰，曽根智史，笹島　茂，佐々木昌弘他	第17巻　第10章『医療制度・医療政策・医療経済』		シリーズ生命倫理　全20巻	丸善出版	日　本	2013．２．２８	170-191
烏帽子田彰 加藤眞三	ｱﾙｺｰﾙによる身体疾患（第６章）		ｱﾙｺｰﾙ白書	財〉ｱﾙｺｰﾙ健康医学協会		2013	13-15
Yasuno F	Effect of plasma lipids and APOE genotype on cognitive decline.		Triglycerides:Chemical -Structure, Biosynthesis and Role in Disease	NOVA SCIENCE		2013	140-167

安野史彦	器質性健忘症候群、アルコールおよび他の精神作用物質によらないもの		ＩＣＤ－１０精神科診断ガイドブック	中山書店	東京	2013	78-86

雑誌

発表者氏名	論文タイトル名	発表誌名	巻号	ページ	出版年
Kobayashi Z, Arai T, Yokota O, Tsuchiya K, Hosokawa M, Oshima K, Niizato K, Akiyama H, Mizusawa H	Atypical FTLD-FUS associated with ALS-TDP: a case report.	Neuropathology	33	83-86	2013
Masuda-Suzukake M, Nonaka T, Hosokawa M, Oikawa T, Arai T, Akiyama H, Mann D, Hasegawa M	Prion-like spreadding of pathological alpha-synuclein in brain.	Brain	136	1128-1138	2013
Nonaka T, Masuda-Suzukake M, Arai T, Hasegawa Y, Akatsu H, Obi T, Yoshida M, Murayama S, Mann DMA, Akiyama H, Hasegawa M	Prion-like properties of pathological TDP-43 aggregates from diseased brains.	Cell Rep	4	124-134	2013
Kobayashi Z, Kawakami I, Arai T, Yokota O, Tsuchiya K, Kondo H, Shimomura Y, Haga C, Aoki N, Hasegawa M, Hosokawa M, Oshima K, Niizato K, Ishizu H, Terada S, Onaya M, Ikeda M, Oyanagi K, Nakano I, Murayama S, Akiyama H, Mizusawa H	Pathological features of FTLD-FUS in a Japanese population: Analyses of nine cases.	J Neurol Sci	335	89-95	2013
Kobayashi Z, Akaza M, Ishihara S, Tomimitsu H, Inadome Y, Arai T, Akiyama H, Shintani S	Thalamic hypoperfusion in early stage of progressive supranuclear palsy (Richardson's syndrome): Report of an autopsy-confirmed case.	J Neurol Sci	335	224-227	2013
Liu R, Yang G, Nonaka T, Arai T, Jia W, Cynader MS	Reducing TDP-43 aggregation does not prevent its cytotoxicity.	Acta Neuropathol Commun	1	49	2013

新井哲明	認知症性疾患の病理・分子対応	Cognition and Dementia	12	48-55	2013
細川雅人, 新井哲明	前頭側頭葉変性症の病理と関連遺伝子	Clinical Neuroscinece	12	1435-1437	2013
Ikeda M, Mori E, Kosaka K, Iseki E, Hashimoto M, Matsukawa N, Matsuo K, Nakagawa M, on behalf of the Donepezil-DLB Study Investigators	Long-term safety and efficacy of Donepezil in patients with dementia with Lewy Bodies: Results from a 52-week, open-label, multicenter extension study.	Dement Geriatr Cogn Disord	36(3-4)	229-241	2013
Yatabe Y, Hashimoto M, Kaneda K, Honda K, Ogawa Y, Yuuki S, Ikeda M	Efficacy of increasing donepezil in mild to moderate Alzheimer's disease patients who show a diminished response to 5 mg donepezil: a preliminary study.	Psychogeriatrics	13(2)	88-93	2013
Hasegawa N, Hashimoto M, Yuuki S, Honda K, Yatabe Y, Araki K, Ikeda M	Prevalence of delirium among outpatients with dementia.	Int Psychoteriatr	25(11)	1877-1883	2013
Ichimi N, Hashimoto M, Matsushita M, Yano H, Yatabe Y, Ikeda M	The relationship between primary progressive aphasia and neurodegenerative dementia.	East Asian Arch Psychiatry	23(3)	120-125	2013
Adachi H, Ikeda M, Komori K, Shinagawa S, Toyota Y, Kashibayashi T, Ishikawa T, Tachibana N	Comparison of the utility of everyday memory test and the Alzheimer's Disease Assessment Scale-Cognitive part for evaluation of mild cognitive impairment and very mild Alzheimer's disease.	Psychiatry Clin Neurosci	67(3)	148-153	2013
Honda K, Hashimoto M, Yatabe Y, Kaneda K, Yuki S, Ogawa Y, Matsuzaki S,Tsuyuguchi A, Tanaka H, Kashiwagi H, Hasegawa N, Ishikawa T, Ikeda M	The usefulness of monitoring sleep talking for the diagnosis of dementia with Lewy bodies.	Int Psychogeriatrics	25	851-858	2013

橋本　衛, 池田　学	認知症ガイドライン　１．アルツハイマー病	画像診断	33(10)	1167-1181	2013
Hitoshi Okamura Shinya Ishii Tomoyuki Ishii Eboshida Akira	Prevalence of dementia in Japan: a systematic review	Dement Geriatr Cogn Disord	Vol. 36	pp 111-118	2013
北村　立	認知症の早期対応と生活支援について	日本未病システム学会雑誌	19巻2号	41-45	2013
北村　立、長谷川　静子	認知症の行動制限を考える　—身体拘束を中心に—	精神科治療学	28巻10号	1301-1306	2013
Hatano Y, Narumoto J, Shibata K, Matsuoka T, Taniguchi S, Hata Y, Yamada K, Yaku H, Fukui K.	White matter hyperintensities predict delirium after cardiac surgery.	Am J Geriatr psychiatry.	21(10)	938-45	2013
Taniguchi S, Narumoto J, Shibata K, Ayani N, Matsuoka T, Okamura A, Nakamura K, Shimizu H, Fukui K.	Treatment in a ward for elderly patients with dementia in Japan.	Neuropsychiatr Dis Treat	9	357-63	2013
Kato Y, Narumoto J, Matsuoka T, Okamura A, Koumi H, Kishikawa Y, Terashima S, Fukui K.	Diagnostic performance of a combination of Mini-Mental State Examination and Clock Drawing Test in detecting Alzheimer's disease.	Neuropsychiatr Dis Treat	9	581-6	2013
Matsuoka T, Narumoto J, Okamura A, Taniguchi S, Kato Y, Shibata K, Nakamura K, Okuyama C, Yamada K, Fukui K.	Neural correlates of the components of the clock drawing test.	Int Psychogeriatr	25	1317-1323	2013
Iida N, Shibata K, Nagahara Y, Okamura A, Matsuoka T, Nakamae T, Narumoto J, Fukui K.	Case of dementia with Lewy bodies that progressed from schizoaffective disorder.	Psychiatry Clin Neurosci.	67(4)	281-282	2013

加藤佑佳，松岡照之，小川真由，谷口将吾，藤本宏，占部美恵，柴田敬祐，中村佳永子，江口洋子，飯干紀代子，小海宏之，仲秋秀太朗，三村　將，福居顯二，成本　迅.	認知機能障害により医療行為における同意能力が問題となった2例-MacCAT-Tを用いた医療同意能力の評価について-.	老年精神医学雑誌	24	928-936	2013
Yasuno F , Matsuoka K, Kitamura S, a Kiuchi K, Kosaka J, Okada K, Tanaka S, Shinkai T, Taoka T, Kishimoto T.	Decision-making deficit of a patient with axonal damage after traumatic brain injury	Brain Cog	84	63-82	2014
Kitamura S, Kiuchi K, Taoka T, Hashimoto K, Ueda S, Yasuno F, Morikawa M, Kichikawa K, Kishimoto T	Longitudinal white matter changes in Alzheimer's disease: a tractography-based analysis study.	Brain Res	515	12-18	2013
Yasuno F, Asada T.	Effect of plasma lipids and APOE genotype on cognitive decline.	Dialogues Clin Neurosci	15	120-126	2013
Nose M, Kodama C, Ikejima C, Mizukami K, Matsuzaki A, Tanaka S, Yoshimura A, Yasuno F, Asada T	ApoE4 is not associated with depression when mild cognitive impairment is considered	Int J Geriatr Psychiatry	28	155-163	2013
安野史彦	神経・精神症候からのアプローチ　主要神経・精神症候と鑑別診断 せん妄　意識が混濁し、幻覚や錯覚がみられる	日本医師会雑誌	142	122-123	2013
数井 裕光，田中 稔久，安野 史彦，武田 雅俊	アルツハイマー病の早期診断における臨床診断基準と神経心理検査の有用性	Dementia Japan	27	316-323	2013
安野史彦	脳梗塞と精神症状	奈良県医師会医学会年報	26	35-40	2013
安野史彦	認知症の予防　「SCI・MCI」	精神科	22	410-417	2013

Ⅳ. 研究成果の刊行物・別刷

NEUROPATHOLOGY

Neuropathology 2013; **33**, 83–86 doi:10.1111/j.1440-1789.2012.01325.x

Case Report

Atypical FTLD-FUS associated with ALS-TDP: A case report

Zen Kobayashi,[1,2] Tetsuaki Arai,[1,4] Osamu Yokota,[5] Kuniaki Tsuchiya,[1] Masato Hosokawa,[1] Kenichi Oshima,[3] Kazuhiro Niizato,[3] Haruhiko Akiyama[1] and Hidehiro Mizusawa[2]

[1]Dementia Research Project, Tokyo Metropolitan Institute of Medical Science, [2]Department of Neurology and Neurological Science, Graduate School, Tokyo Medical and Dental University, [3]Tokyo Metropolitan Matsuzawa Hospital, Tokyo, [4]Department of Psychiatry, Graduate School of Comprehensive Human Sciences, University of Tsukuba, Ibaraki and [5]Department of Neuropsychiatry, Okayama University Graduate School of Medicine, Dentistry and Pharmaceutical Sciences, Okayama, Japan

A 30-year-old Japanese woman without relevant family history presented with a behavioral abnormality followed by motor weakness about 14 years later. The patient died at age 45. Post mortem examination revealed degeneration of the frontal and temporal lobes, as well as lower motor neurons in the brainstem and spinal cord. These features were reported previously as being consistent with a diagnosis of frontotemporal lobar degeneration (FTLD) with amyotrophic lateral sclerosis (ALS). In the present study, we show abundant fused in sarcoma (FUS)-positive dystrophic neurites but only a few neuronal cytoplasmic inclusions in the frontal and temporal cortices. TAR DNA-binding protein 43 (TDP-43)-positive inclusions were absent in the cerebrum. However, TDP-43-positive inclusions were present in the lower motor neurons of the brainstem and spinal cord. To our knowledge, this is the first report of a case in which FTLD-FUS pathology is of a dystrophic neurites-predominant type and FTLD-FUS is associated with ALS-TDP.

Key words: amyotrophic lateral sclerosis, dystrophic neurites, frontotemporal lobar degeneration, FUS, neuronal cytoplasmic inclusions, TDP-43.

INTRODUCTION

In frontotemporal lobar degeneration (FTLD) with fused in sarcoma (FUS) accumulation (FTLD-FUS) and FTLD with TAR DNA-binding protein 43 (TDP-43) accumulation (FTLD-TDP), aggregates of pathological proteins occur principally in two forms, neuronal cytoplasmic inclusions (NCI) and dystrophic neurites (DN). There is a pathological subtype of FTLD-TDP in which DNs are the predominant form of TDP-43 accumulation in the cerebral cortex. However, thus far there has been no report of DN-predominant pathology in FTLD-FUS.[1–5] We describe here a case associated with DN-predominant accumulation of FUS in the cerebral cortex.

CASE

In 2001, one of us (KT) reported an autopsy case of unusual FTLD.[6] The patient developed a behavioral variant of frontotemporal dementia (bvFTD) at age 30. Approximately 14 years later, she showed symptoms and signs of amyotrophic lateral sclerosis (ALS). Post mortem examination revealed atrophy of the frontal and temporal lobes. Atrophy was particularly evident in the convexity of the frontal lobes and in the caudate nucleus (Fig. 1A). Ubiquitin immunohistochemistry demonstrated NCI in the cerebral cortex and amygdala. In the hippocampal dentate gyrus, a small number of DN were seen but no NCI or neuronal intranuclear inclusions (NII) were found.[6]

In the present study, we re-examined this case with immunohistochemistry using the following antibodies: anti-α-internexin (Santa Cruz Biotechnology, Santa Cruz, CA, USA: 2E3), anti-TDP-43 (Proteintech, Chicago, IL, USA, 10782-2-AP), anti-phosphorylated TDP-43 (pS403/404),[7] and anti-FUS (Sigma-Aldrich, St Louis, MO, USA, HPA008784 and Proteintech, 11570-1-AP). Sections were pretreated by autoclaving for 10 min in 10 mmol sodium citrate buffer, pH 6.0, at 120°C.

Correspondence: Haruhiko Akiyama, Project Leader, Dementia Research Project, Tokyo Metropolitan Institute of Medical Science, 2-1-6 Kamikitazawa, Setagaya-ku, Tokyo 156-8506, Japan. Email: akiyama-hr@igakuken.or.jp

Received 9 March 2012; revised and accepted 5 April 2012; published online 29 May 2012.

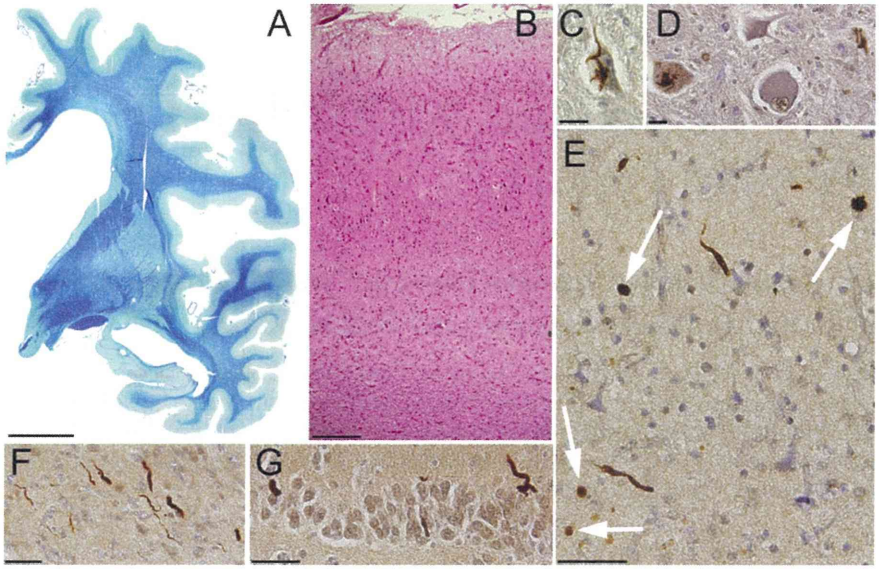

Fig. 1 (A) The left hemisphere showing atrophy of the frontal and temporal cortices and the caudate nucleus. KB staining. (B) HE staining of the entire depth of the frontal cortex. Tissue rarefaction is evident, particularly in the deep layers. (C) A TAR DNA-binding protein 43 (TDP-43)-positive skein-like inclusion in the motor nucleus of the trigeminal nerve. (D) TDP-43-positive inclusions in the spinal cord. (E) Fused in sarcoma (FUS)-positive dystrophic neurites (DN) and dot-like structures (arrows) in the superficial layers of the frontal cortex. (F) FUS-positive DN in the deep layers of the frontal cortex. (G) FUS-positive DN in the hippocampal dentate gyrus. Scale bars = 1 cm (A), 200 μm (B), 20 μm (C, D) and 50 μm (E–G).

In the cerebral cortex, degeneration was more severe in the deep layers than in the superficial layers (Fig. 1B). In subcortical structures, neuronal loss was evident in the caudate nucleus, amygdala, hypoglossal nucleus, dorsal vagal nucleus and spinal cord anterior horn (Table 1). As reported previously, we were not able to confirm the presence of Bunina bodies by HE staining. Apparent NCIs were not visible by HE staining or by α-internexin immunostaining.

A characteristic feature of this case was the accumulation of TDP-43 and FUS in distinct regions of the CNS. TDP-43-positive NCI occurred in the substantia nigra, trochlear nucleus, motor nucleus of the trigeminal nerve (Fig. 1C) and hypoglossal nucleus, as well as in the spinal cord anterior horn (Fig. 1D). TDP-43-positive glial cytoplasmic inclusions (GCI) were also present in all of these regions except for the trochlear nucleus. TDP-43 accumulation was absent in the cerebrum. In contrast, FUS-positive NCI and DN were seen in the cerebral cortex as well as in some subcortical structures. In the cerebral cortex and caudate nucleus, FUS-positive DN predominated over NCI. FUS immunostaining revealed far more numerous DN than did ubiquitin immunostaining. In addition to DN, FUS-positive dot-like structures were seen in the neuropil. The dot-like structures were present mainly in the cortical superficial layers (Fig. 1E), whereas the DNs were frequent in the deep layers (Fig. 1F). In the hippocampal dentate gyrus, a small number of DNs were found but no NCIs or NIIs were seen (Fig. 1G). In the subcortical structures, accumulation of FUS occurred in the caudate nucleus, amygdala, locus coeruleus and periaqueductal gray matter. FUS accumulation was absent in the medulla oblongata and spinal cord. FUS-positive GCIs were not found. The distribution and the degree of TDP-43 and FUS accumulation are summarized in Table 1. Occurrence of abnormal protein aggregates generally paralleled the severity of degenerative changes.

DISCUSSION

In the present case, both TDP-43 and FUS were deposited in a single patient. However, the distribution was entirely different. A recent article described association of FUS with TDP-43 accumulation in sporadic ALS.[8] We were not able to find any overlap between the accumulation of FUS and TDP-43 in this patient. The long interval of more than a decade between the occurrence of bvFTD and ALS suggests that the TDP-43 pathology may not be relevant to the preceding FUS pathology. Therefore, the current neuropathological diagnosis of this case would be FTLD-FUS complicated with ALS-TDP, although such a situation should be extremely rare.

In addition, it has to be noted that this case is atypical of FTLD-FUS. Degenerative changes were relatively mild in the putamen, globus pallidus, hippocampal CA1 and dentate gyrus, subiculum and entorhinal cortex compared with typical FTLD-FUS cases. In such areas, FUS accumulation was also mild. More importantly, FUS accumulation occurred predominantly in the form of DN in the cerebral cortex, hippocampal dentate gyrus and caudate nucleus. To our knowledge, no report has been made so far on FTLD-FUS cases with DN-predominant pathology. Recently, the morphology of abnormal FUS accumulations has been described in detail for each neuropathological subtype of FLTD-FUS.[2] Our case does not seem to match any previously described subtypes. Obviously, there is a need for

Table 1 Distribution and severity of CNS lesions

	FUS+ DN	FUS+ dots	FUS + NCI	TDP-43+ NCI	Degeneration
Superior frontal gyrus (ant./post.)	4/3	3/2	2/2	0/n	+++/+++
Middle frontal gyrus (ant./post.)	3/2	2/2	1/2	0/n	+++/+++
Inferior frontal gyrus (ant.)	4	3	2	0	+++
Orbital gyrus	3	3	2	0	+++
Primary motor cortex	3	3	1	0	++
Superior temporal gyrus (mid/post.)	1/1	1/1	1/2	n/0	+/±
Middle temporal gyrus (mid/post.)	2/2	2/2	1/2	n/0	++/+
Inferior temporal gyrus (mid/post.)	2/2	2/2	1/2	n/0	++/+
Postcentral gyrus	1	1	1	0	+
Supramarginal gyrus	2	2	2	0	+
Insular cortex	3	2	2	0	+++
Cingulate gyrus (ant./post.)	4/2	4/3	2/2	n/0	++/++
Amygdala	1	2	2	n	++
Ambient gyrus	3	2	1	n	++
Hippocampal CA1	1	0	0	0	-
Hippocampal dentate gyrus	2	1	0	0	-
Subiculum	1	0	1	0	+
Entorhinal cortex	2	2	2	0	+
Transentorhinal cortex	2	3	2	0	++
Caudate nucleus	1	3	1	0	+++
Putamen	0	0	0	0	+‡
Globus pallidus	0	0	0	n	+‡
Thalamus†	0	0	0	0	+
Lateral mamillary nucleus	4	3	0	n	+
Nucleus basalis of Meynert	0	1	0	n	+‡
Cerebellar dentate nucleus	n	n	n	n	±
Periaqueductal gray matter	1	1	1	0	±
Oculomotor nucleus	n	n	n	n	±
Trochlear nucleus	0	0	0	3	–
Red nucleus	n	n	n	n	±
Substantia nigra	0	0	0	1	+
CST at the level of midbrain	n	n	n	n	+
FPT at the level of midbrain	n	n	n	n	–
Locus ceruleus	0	0	2	0	–
Pontine nucleus	0	0	0	0	±
Motor nucleus of trigeminal nerve	0	0	0	3	+
CST at the level of pons	n	n	n	n	+
Dorsal vagal nucleus	0	0	0	0	++
Hypoglossal nucleus	0	0	0	3	+++
Inferior olivary nucleus	0	0	0	0	±
Pyramid	n	n	n	n	+
Anterior horn of spinal cord	0	0	0	3	++
CST of spinal cord	n	n	n	n	+

The degree of TDP-43 and FUS accumulation was assessed according to the grading system employed by Neumann *et al.*[5] FUS, fused in sarcoma; TDP-43, TAR DNA-binding protein 43; DN, dystrophic neurite; dots, dot-like structures; NCI, neuronal cytoplasmic inclusion; ant., anterior portion; post., posterior portion; mid, middle portion; CST corticospinal tract; FPT, frontopontine tract; n, not available or not evaluated. The severity of degeneration in the gray matter: –, no degeneration; ±, no neuronal loss but gliosis; +, slight neuronal loss; ++, moderate neuronal loss; +++, severe neuronal loss. Degeneration in the white matter: +, present; -, absent. †The region other than the lateral mamillary nucleus was evaluated. ‡Remaining neurons showed atrophy suggestive of anoxic changes. The cerebrum was evaluated in the left hemisphere.

further, extensive analyses of many cases for abnormal accumulation of FUS and TDP-43.

ACKNOWLEDGMENT

We thank Ms. Hiromi Kondo, Ms. Chie Haga and Ms. Yoko Shimomura for their excellent work on tissue preparation and staining. This research was supported by Grants-in-Aid from the Ministry of Health, Labor and Welfare, Japan, 10102894 and 10103470 (HA), and the Ministry of Education, Culture, Science 09019658 (HA). None of the authors has any conflict of interest.

REFERENCES

1. Armstrong RA, Gearing M, Bigio EH *et al.* The spectrum and severity of FUS-immunoreactive inclusions in the frontal and temporal lobes of ten cases of neuronal intermediate filament inclusion disease. *Acta Neuropathol* 2011; **12**: 219–228.

2. Mackenzie IR, Munoz DG, Kusaka H *et al.* Distinct pathological subtypes of FTLD-FUS. *Acta Neuropathol* 2011; **121**: 207–218.
3. Munoz DG, Neumann M, Kusaka H *et al.* FUS pathology in basophilic inclusion body disease. *Acta Neuropathol* 2009; **118**: 617–627.
4. Neumann M, Rademakers R, Roeber S, Baker M, Kretzschmar HA, Mackenzie IR. A new subtype of frontotemporal lobar degeneration with FUS pathology. *Brain* 2009; **132**: 2922–2931.
5. Neumann M, Roeber S, Kretzschmar HA, Rademakers R, Baker M, Mackenzie IR. Abundant FUS-immunoreactive pathology in neuronal intermediate filament inclusion disease. *Acta Neuropathol* 2009; **118**: 605–616.
6. Tsuchiya K, Ikeda K, Haga C *et al.* Atypical amyotrophic lateral sclerosis with dementia mimicking frontal Pick's disease: a report of an autopsy case with a clinical course of 15 years. *Acta Neuropathol* 2001; **101**: 625–630.
7. Hasegawa M, Arai T, Nonaka T *et al.* Phosphorylated TDP-43 in frontotemporal lobar degeneration and amyotrophic lateral sclerosis. *Ann Neurol* 2008; **64**: 60–70.
8. Deng HX, Zhai H, Bigio EH *et al.* FUS-immunoreactive inclusions are a common feature in sporadic and non-SOD1 familial amyotrophic lateral sclerosis. *Ann Neurol* 2010; **67**: 739–748.

doi:10.1093/brain/awt037 Brain 2013: 136; 1128–1138 | 1128

BRAIN
A JOURNAL OF NEUROLOGY

Prion-like spreading of pathological α-synuclein in brain

Masami Masuda-Suzukake,[1] Takashi Nonaka,[1] Masato Hosokawa,[2] Takayuki Oikawa,[1] Tetsuaki Arai,[3] Haruhiko Akiyama,[2] David M.A. Mann[4] and Masato Hasegawa[1]

1 Department of Neuropathology and Cell Biology, Tokyo Metropolitan Institute of Medical Science, 2-1-6 Kamikitazawa, Setagaya-ku, Tokyo 156-8506, Japan
2 Dementia Research Project, Tokyo Metropolitan Institute of Medical Science, 2-1-6 Kamikitazawa, Setagaya-ku, Tokyo, 156-8506, Japan
3 Department of Psychiatry, Graduate School of Comprehensive Human Sciences, University of Tsukuba, 1-1-1, Tennodai, Tsukuba, Ibaraki 305-8575, Japan
4 Centre for Clinical and Cognitive Neuroscience, Institute of Brain Behaviour and Mental Health, University of Manchester, Salford M6 8HD, Manchester, UK

Correspondence to: Masato Hasegawa, Ph.D.
Department of Neuropathology and Cell Biology,
Tokyo Metropolitan Institute of Medical Science,
2-1-6 Kamikitazawa, Setagaya-ku,
Tokyo 156-8506,
Japan
E-mail: hasegawa-ms@igakuken.or.jp

α-Synuclein is the major component of filamentous inclusions that constitute the defining characteristic of neurodegenerative α-synucleinopathies. However, the molecular mechanisms underlying α-synuclein accumulation and spread are unclear. Here we show that intracerebral injections of sarkosyl-insoluble α-synuclein from brains of patients with dementia with Lewy bodies induced hyperphosphorylated α-synuclein pathology in wild-type mice. Furthermore, injection of fibrils of recombinant human and mouse α-synuclein efficiently induced similar α-synuclein pathologies in wild-type mice. C57BL/6J mice injected with α-synuclein fibrils developed abundant Lewy body/Lewy neurite-like pathology, whereas mice injected with soluble α-synuclein did not. Immunoblot analysis demonstrated that endogenous mouse α-synuclein started to accumulate 3 months after inoculation, while injected human α-synuclein fibrils disappeared in about a week. These results indicate that α-synuclein fibrils have prion-like properties and inoculation into wild-type brain induces α-synuclein pathology *in vivo*. This is a new mouse model of sporadic α-synucleinopathy and should be useful for elucidating progression mechanisms and evaluating disease-modifying therapy.

Keywords: α-synuclein; Lewy bodies; Parkinson's disease; propagation

Introduction

Filamentous inclusions composed of α-synuclein in nerve cells or glial cells are the defining neuropathological feature of a group of neurodegenerative diseases including Parkinson's disease, dementia with Lewy bodies, and multiple-system atrophy (Goedert, 2001). In these so-called α-synucleinopathies, α-synuclein is deposited in a hyperphosphorylated form with β-sheet-rich, fibrillar structure (Spillantini *et al.*, 1997, 1998; Baba *et al.*, 1998; Wakabayashi *et al.*, 1998; Fujiwara *et al.*, 2002). Missense mutations (A30P, E46K and A53T) in the α-synuclein gene (Polymeropoulos *et al.*, 1997; Kruger *et al.*, 1998; Zarranz *et al.*, 2004) and multiplications of the region (Singleton *et al.*, 2003; Chartier-Harlin *et al.*, 2004; Ibanez *et al.*, 2004,) have been identified in familial forms of Parkinson's disease and dementia with Lewy bodies, indicating that abnormalities of α-synuclein cause

Received November 24, 2012. Revised January 11, 2013. Accepted January 14, 2013. Advance Access publication March 6, 2013

these diseases. Neuropathologically, α-synuclein lesions are believed to spread progressively throughout the brain and their spread correlates to the staging of clinical symptoms (Muller *et al.*, 2005), as in the case of tau pathology in Alzheimer's disease (Braak and Braak, 1991). Kordower *et al.* (2008) and Li *et al.* (2008) reported that embryonic neurons transplanted into the striatum of an individual with Parkinson's disease developed Lewy body-like pathologies, suggesting that pathological α-synuclein may be transmissible from diseased neurons to healthy neurons. Recent studies have also shown that exogenous α-synuclein fibrils induced Lewy body pathology in cultured neurons (Desplats *et al.*, 2009; Emmanouilidou *et al.*, 2010; Nonaka *et al.*, 2010; Volpicelli-Daley *et al.*, 2011), transgenic mouse brain (Mougenot *et al.*, 2012; Luk *et al.*, 2012*b*) and wild-type mouse brain (Luk *et al.*, 2012*a*). In addition, a growing body of evidence indicates that self-propagating protein aggregates play central roles in many neurodegenerative diseases, including Parkinson's disease and Alzheimer's disease (Clavaguera *et al.*, 2009; Mougenot *et al.*, 2012; Luk *et al.*, 2012*b*; Stohr *et al.*, 2012). In this work, we have tested whether inoculation of insoluble α-synuclein from brains with dementia with Lewy bodies and synthetic mouse and human α-synuclein fibrils can induce α-synuclein pathology in wild-type mice. As a result, we have established a new mouse model of sporadic α-synucleinopathy using wild-type mice.

Materials and methods

Preparation of recombinant α-synuclein monomer and fibrils

Human and mouse α-synuclein were expressed in *E. coli* BL21 (DE3) cells, as described (Masuda *et al.*, 2006*b*). To avoid the production of α-synuclein dimers induced by misexpression of cysteine-containing α-synuclein, the Y136-TAT construct was used (Masuda *et al.*, 2006*a*). α-Synuclein was purified by boiling, Q-Sepharose® ion exchange chromatography and ammonium sulphate precipitation, before dialysis against 30 mM Tris–HCl, pH 7.5. Recombinant proteins were centrifuged at 113 000*g* for 20 min at 4°C to remove insoluble materials and used as α-synuclein monomer. Protein concentrations were determined as described (Yonetani *et al.*, 2009). Purified human and mouse α-synuclein (7 mg/ml) were incubated at 37°C in a shaking incubator (200 rpm) in 30 mM Tris–HCl, pH 7.5, containing 0.1% NaN_3, for 72 h. α-Synuclein fibrils were pelleted by spinning the assembly mixtures at 113 000*g* for 20 min.

Preparation of the insoluble fraction of dementia with Lewy bodies brain

Fresh frozen brain tissue from a patient with dementia with Lewy bodies (phosphorylated α-synuclein pathology is shown in Supplementary Fig. 9) was homogenized in 18 volumes (w/v) of Buffer A (10 mM Tris-HCl, pH 7.4, 0.8 M NaCl, 1 mM EGTA, and 10% sucrose), and sarkosyl was added to the homogenate at a concentration of 2%. The mixture was incubated for 30 min at 37°C, sonicated and spun at 9100*g* for 10 min at 25°C. The supernatant was further centrifuged at 113 000*g* for 20 min at 25°C, and the sarkosyl-insoluble pellet was washed with Buffer A. The pellet was taken up in saline, sonicated and centrifuged at 800*g* for 5 min. The supernatant was used for stereotaxic injection.

Stereotaxic surgery

Four- to six-month-old female C57BL/6J mice (CLEA Japan, Inc.) anaesthetized with 50 mg/kg pentobarbital sodium were injected with 10 μg of recombinant α-synuclein monomer, fibrils or 5 μl of insoluble fraction of dementia with Lewy bodies brain into substantia nigra (anterior-posterior: −3.0 mm; medial-lateral: −1.3 mm; dorsal-ventral: −4.7 mm from the bregma and dura) using a 10-μl Hamilton syringe. Mice were anaesthetized with isoflurane and killed by decapitation. For immunohistochemistry, brains were fixed in 10% formalin neutral buffer solution (Wako), and for biochemical analysis, brains were snap-frozen on dry ice and stored at −80°C. All experimental protocols were approved by the Animal Care and Use Committee of the Tokyo Metropolitan Institute of Medical Science.

Immunohistochemistry

Brains fixed in 10% formalin were cut on a vibratome (Leica) at 50 μm thickness. The free-floating sections were treated with 0.5% H_2O_2 in methanol for 30 min to inactivate peroxidase and blocked with 10% calf serum in PBS. Sections were immunostained with appropriate antibodies. Antibodies used in this study are summarized in Supplementary Table 1. After incubation with the biotinylated-secondary antibody (Vector), labelling was detected using the ABC staining kit (Vector).

Confocal microscopy

For double-label immunofluorescence for phosphorylated α-synuclein and ubiquitin or phosphorylated α-synuclein and p62, brain sections were incubated overnight at 4°C in a cocktail of 1175 and anti-ubiquitin or anti-p62 antibody. The sections were then washed and incubated in a cocktail of Alexa Fluor® 568-conjugated goat anti mouse IgG (Molecular Probes) and Alexa Fluor® 488-conjugated goat anti mouse IgG (Molecular Probes). After further washing, sections were stained with TO-PRO®-3, coverslipped with VECTASHIELD® (Vector) and observed with a laser-scanning confocal fluorescence microscope (LSM5 PASCAL, Carl Zeiss).

Biochemical analysis

Mouse brains were homogenized in 20 volumes (w/v) of Buffer A, then spun at 100 000*g* for 30 min at 4°C, and the supernatant was retained as buffer-soluble fraction. The pellet was homogenized in 20 volumes of Buffer A containing 1% Triton™ X-100 and incubated for 30 min at 37°C. After centrifugation at 100 000*g*, the Triton™-insoluble pellet was further homogenized in Buffer A containing 1% sarkosyl and incubated at 37°C for 30 min. Samples were spun at 100 000*g* for 30 min. The sarkosyl-pellet was sonicated in 30 mM Tris-HCl, pH 7.4, and used for immunoblotting as sarkosyl-insoluble fraction. The samples were subjected to SDS-PAGE on 12.5% polyacrylamide gel and proteins were electrotransferred onto a polyvinylidene difluoride membrane, probed with appropriate antibodies and detected as described (Nonaka *et al.*, 2009).

Behavioural tests

Open field test

Each mouse was placed in the centre of the open field apparatus (25-cm diameter). Activity was measured by SUPERMEX system (Muromachi Kikai) over 90-min period and analysed by CompACT AMS software ver.3 (Muromachi Kikai). Total activity was measured by counting the number of photobeam interruptions over every 5-min period.

Wire hang test

Neuromuscular strength was tested with a wire hang test. The mouse was placed on a wire mesh, waved gently so that the mouse gripped the wire and then inverted. Latency to fall was recorded with a 300-s cut-off time.

Rotarod test

The Rotarod test, using an accelerating Rotarod (Muromachi Kikai), was performed by placing mice on 9-cm diameter rods and measuring the time each animal was able to maintain its balance on the rod. We used 9-cm rods to make the test more sensitive to motor skill learning (Shiotsuki *et al.*, 2010). The speed of the rotarod accelerated from 0 to 40 rpm over a 5-min period.

Y-maze test

Y-maze apparatus (Muromachi Kikai) consisted of three arms (40 cm × 3 cm) made of grey plastic joined in the middle to form a Y shape. Mice were placed into one of the arms of the maze and allowed to explore freely the maze for an 8-min session. The alternation between arms was recorded.

Intranasal administration of abnormal α-synuclein fibrils

Twenty micrograms of recombinant α-synuclein monomer or preformed fibrils, or 10 μl of insoluble fraction of dementia with Lewy bodies brain, was administered intranasally once a week for 1 month to 10-week-old female C57BL/6J mice (soluble mouse α-synuclein, soluble human α-synuclein, mouse α-synuclein fibrils, human α-synuclein fibrils and dementia with Lewy bodies extracts, $n = 5$ per group). At 21 months after the last administration, mice were anaesthetized with pentobarbital sodium and killed by perfusion with phosphate buffer (pH 7.4) and 4% paraformaldehyde in 0.1% phosphate buffer. Brains were cryosectioned and immunostained as described above.

Results

To investigate whether insoluble α-synuclein fibrils can propagate *in vivo*, we injected recombinant human α-synuclein fibrils into the substantia nigra in the right cerebral hemisphere of C57BL/6J mice. α-Synuclein fibrils were prepared using highly purified recombinant α-synuclein (Supplementary Fig. 1A) by incubation with shaking. Formation of the fibrils was confirmed by electron microscopy (Supplementary Fig. 1B) and thioflavin S assay (data not shown). The fibrils were then collected by ultracentrifugation, sonicated and used for injection. Abnormal phosphorylated α-synuclein-positive structures were observed in the brains of mice injected with human α-synuclein fibrils at 15 months after inoculation (Fig. 1). Phosphorylated α-synuclein pathology was distributed throughout the brain including substantia nigra, amygdala, dentate gyrus, hippocampal CA1-3, molecular layer of hippocampus, fimbria, stria terminalis, hypothalamus, somatosensory area, visual cortex, cingulate cortex and corpus callosum (Fig. 1). Phosphorylated α-synuclein-positive structures were also positive for anti-ubiquitin and p62 antibodies (Fig. 2A). Co-localization was confirmed by confocal microscopy (Fig. 2B and C), indicating that these structures have the same immunoreactive properties as Lewy bodies (Kuusisto *et al.*, 2001). By contrast, no phosphorylated α-synuclein, ubiquitin or p62-positive pathology was observed in the brains of mice injected with soluble human α-synuclein (Supplementary Fig. 2). Remarkably, despite the unilateral injection of α-synuclein fibrils, phosphorylated α-synuclein-positive pathology appeared bilaterally (Fig. 3A). In the right hemisphere (injected side), phosphorylated α-synuclein pathology was seen abundantly in dentate gyrus and amygdala, whereas in the left hemisphere no pathology was seen in amygdala and only sparsely in dentate gyrus (Fig. 3A). These results strongly suggest that α-synuclein pathology propagates throughout the brain from the injection site. To understand the spreading pathway of phosphorylated α-synuclein pathology, we investigated in detail the distribution in four coronal sections at 15 months after inoculation (Fig. 3B). Near the injection level (bregma −3.40 mm), abundant phosphorylated α-synuclein pathology was present in substantia nigra, hippocampus, external capsule and entorhinal cortex in right hemisphere, whereas in the left hemisphere, sparser pathology was detected in hippocampus and external capsule (Fig. 3B). By contrast, at the level of 0.02 mm from bregma (3 mm anterior to the injection level), phosphorylated α-synuclein pathology was concentrated in stria terminalis, septal nucleus and cingulate, motor and somatosensory cortex in the right hemisphere. In the left hemisphere, phosphorylated α-synuclein pathology was detected only in septal nucleus (Fig. 3B). These results suggest that phosphorylated α-synuclein pathology does not spread by simple diffusion and the propensity to accumulate phosphorylated α-synuclein seems to differ among brain regions. The time course of spreading of phosphorylated α-synuclein pathology was analysed by immunohistochemistry and summarized in Table 1. Table 1 clearly indicates that induction of phosphorylated α-synuclein pathology in wild-type mice is time- and brain region-dependent. No signs of astrogliosis and inflammation were observed in human α-synuclein fibril-injected mice compared with soluble-human α-synuclein-injected mice at 15 months after injection (Supplementary Fig. 3).

To clarify which α-synuclein species accumulated in the mice, and when, we performed immunoblot analysis with LB509 and anti-mouse synuclein antibodies, which specifically recognize human α-synuclein and mouse α-synuclein, respectively. The antibody specificities are shown in Supplementary Fig. 1B. At a few

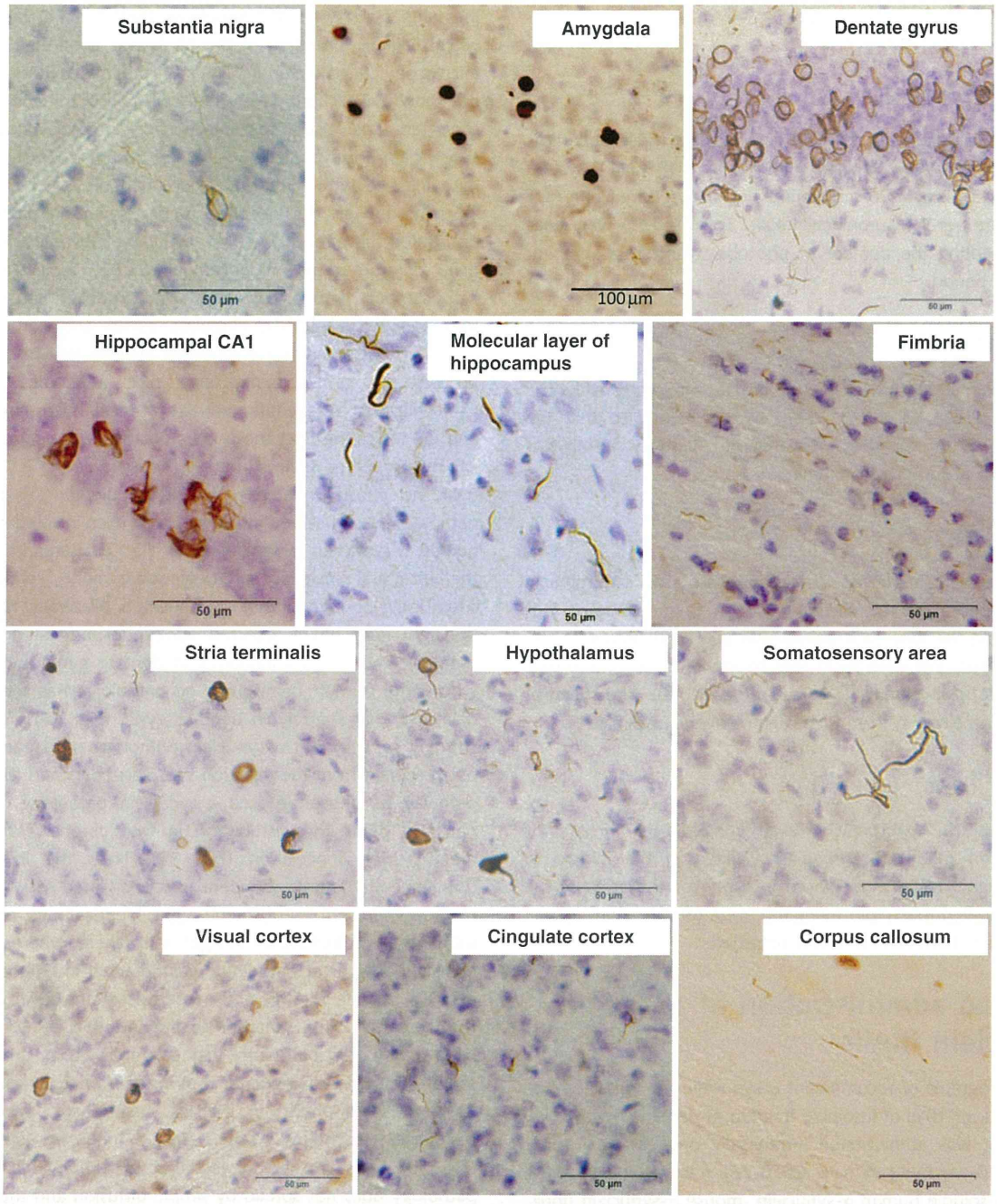

Figure 1 Induction of phosphorylated α-synuclein pathology in wild-type mouse brain injected with human α-synuclein fibrils, observed at 15 months after injection. Sections were immunostained with anti-phosphorylated α-synuclein antibody, 1175. The shapes of phosphorylated α-synuclein-positive structures differed among brain areas. Ring-like and Lewy neurite-like structures were observed in substantia nigra, hippocampus, hypothalamus, somatosensory area, visual cortex, cingulate cortex and corpus callosum, whereas Lewy body- and Lewy neurite-like structures were observed in amygdala and stria terminalis.

hours after injection (Day 0), injected recombinant human α-synuclein fibrils were detected in the sarkosyl-insoluble fraction of the right and left hemispheres by LB509 antibody, suggesting that injected human α-synuclein fibrils in the extracellular space spread quickly throughout the brain. However, at 7 days after injection, the human α-synuclein immunoreactivities had disappeared, and did not reappear at 30 or 90 days after injection (Fig. 4). At 90 days after injection, anti-phosphorylated α-synuclein-positive 15, 20, 30 and 35 kDa bands were detected in the sarkosyl-insoluble fractions. This band pattern is indistinguishable from that of pathological α-synuclein in dementia with Lewy bodies brain (Fig. 4). The 15, 20, 30 and 35 kDa bands correspond to α-synuclein monomer, mono-ubiquitinated α-synuclein, dimer and ubiquitinated dimer, respectively. Most